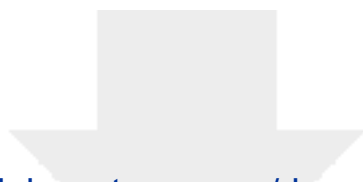


## Effect of Sodium Hydroxide Pretreatment of NiOx Cathodes on the Performance of Squaraine-Sensitized p-Type Dye-Sensitized Solar Cells --Manuscript Draft--

<b>Manuscript Number:</b>	slct.201702867R2
<b>Article Type:</b>	Full Paper
<b>Corresponding Author:</b>	Matteo Bonomo, M.D. La Sapienza Università di Roma Roma, ITALY
<b>Corresponding Author E-Mail:</b>	matteo.bonomo@uniroma1.it
<b>Order of Authors (with Contributor Roles):</b>	Matteo Bonomo, M.D. Andrea Fin Claudio Magistris Roberto Buscaino Claudia Barolo Danilo Dini
<b>Keywords:</b>	p-type DSSC; Squaraines; Nickel Oxide; NIR-adsorber
<b>Manuscript Classifications:</b>	Dyes/Pigments; Photovoltaics; Power sources; Solar cells
<b>Abstract:</b>	Squaraines are full-organic dyes employed as sensitizers in p-type dye-sensitized solar cells (p-DSSC). Their absorption spectrum shows a wide tunability that ranges from visible to NIR. Sensitization in the NIR region is crucial for exploiting a particularly intense portion of the solar spectrum. In this work three squaraines will be presented and tested as sensitizers in NiO-based p-type DSSC O4_C2, O4_C4 and O4_C12). The structures of the dyes differ for the length of the alkyl side chain (C2, C4 and C12). Alkyl side chains improve the solubility of the dye, influence the extent of dye loading on the electrode and affect the overall efficiency of devices. The generally low stability of squaraines represents a critical issue in view of their employment as sensitizers of p-DSSC. Such a problem becomes even more evident when this class of molecules are bound onto an acidic surface like the one of the photocathode here employed: non-stoichiometric nickel oxide (NiOx). NiOx possesses a quite acidic character because of the high surface concentration of Ni(III) sites. To buffer the surface acidity of NiOx due to the presence of high-valence states of nickel, we considered the electrode pretreatment with sodium hydroxide (NaOH) prior to sensitization. This assures a major stability of the solar cell. At the same time the chemisorbed hydroxyl moieties act as passivating agents of the Ni(III) sites thus diminishing the surface concentration of sites for dye anchoring.
<b>Response to Reviewers:</b>	Modification required by the editor have been completed.
<b>Section/Category:</b>	Energy Technology & Environmental Science
<b>Additional Information:</b>	
<b>Question</b>	<b>Response</b>
Submitted solely to this journal?	Yes
Has there been a previous version?	Yes
Please state previous 1) Manuscript ID and 2) journal. 3) If the paper was reviewed, please include a point-by-point response to the reviewer comments. as follow-up to "Has there been a previous version?"	1) cptc.201700191 2) ChemPhotoChem 3) See Attached files: the length of the response to the reviewers is actually longer than 10000 characters.
If accepted, do you wish to publish your	No / Don't know

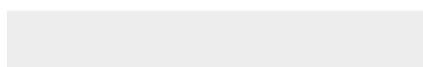
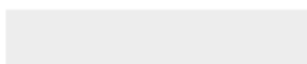
work in an open access format through OnlineOpen?	
Dedication	
Do you or any of your co-authors have a conflict of interest to declare?	No. The authors declare no conflict of interest.
Animal/tissue experiments?	No



Click here to access/download

**Additional Material - Author**

Cover Letter\_ChemistrySelect.docx



# Effect of Sodium Hydroxide Pretreatment of NiO<sub>x</sub> Cathodes on the Performance of Squaraine-Sensitized *p*-Type Dye-Sensitized Solar Cells

Matteo Bonomo,<sup>\*a</sup> Claudio Magistris,<sup>b</sup> Dr. Roberto Buscaino,<sup>b</sup> Dr. Andrea Fin,<sup>c</sup> Prof. Claudia Barolo,<sup>b,d\*</sup> Prof. Danilo Dini<sup>a\*</sup>

a: Department of Chemistry, University of Rome "La Sapienza", p.le Aldo Moro 5, 00139 Rome, Italy

b: Department of Chemistry and NIS Interdepartmental Centre and INSTM Reference Centre, University of Turin, via Pietro Giuria 7, 10125 Torino, Italy

c: Department of Chemistry and Biochemistry, University of California, San Diego, La Jolla, California 92093-0358, United States

d: ICxT Interdepartmental Centre, Lungo Dora Siena 100, 10153, Torino, Italy

\*to whom correspondence should be addressed. E-mail: [bonomo.matteo@uniroma1.it](mailto:bonomo.matteo@uniroma1.it) [claudia.barolo@unito.it](mailto:claudia.barolo@unito.it); [daniilo.dini@uniroma1.it](mailto:daniilo.dini@uniroma1.it)

Squaraines are full-organic dyes employed as sensitizers in *p*-type dye-sensitized solar cells (*p*-DSSC). Their absorption spectrum shows a wide tunability that ranges from visible to NIR. Sensitization in the NIR region is crucial for exploiting a particularly intense portion of the solar spectrum. In this work three squaraines will be presented and tested as sensitizers in NiO-based *p*-type DSSC (**O4\_C2**, **O4\_C4** and **O4\_C12**). The structures of the dyes differ for the length of the alkyl side chain (C2, C4 and C12). Alkyl side chains improve the solubility of the dye, influence the extent of dye loading on the electrode and affect the overall efficiency of devices. The generally low stability of squaraines represents a critical issue in view of their employment as sensitizers of *p*-DSSC. Such a problem becomes even more evident when this class of molecules are bound onto an acidic surface like the one of the photocathode here employed: non-stoichiometric nickel oxide (NiO<sub>x</sub>). NiO<sub>x</sub> possesses a quite acidic character because of the high surface concentration of Ni(III) sites. To buffer the surface acidity of NiO<sub>x</sub> due to the presence of high-valence states of nickel, we considered the electrode pretreatment with sodium hydroxide (NaOH) prior to sensitization. This assures a major stability of the solar cell. At the same time the chemisorbed hydroxyl moieties act as passivating agents of the Ni(III) sites thus diminishing the surface concentration of sites for dye anchoring.

## Introduction

DSSCs have first appeared in 1991<sup>[1]</sup> and since then have represented a frontier technology. The overall device efficiency rose up to 14% over the years due to extensive optimization of several cell parameters<sup>[2]</sup>. Among others, the absorption of the dye is a key factor in DSSC spectral response implying that a strategic design and synthesis of the chromophore is of capital importance to maximize the harvesting of the visible spectra<sup>[3,4]</sup>. Approaches directed to extend the solar light harvesting include the synthesis of dyes with broad absorption bands and/or co-sensitization with molecules that absorb in complementary spectral regions<sup>[5]</sup>. Tandem DSSCs (t-DSSCs) represent one of the most promising approaches, with the combination of two photoelectrodes: a sensitized *n*-type semiconductor as photoanode (e.g. titanium dioxide) and a sensitized *p*-type semiconductor as photocathode (e.g. nickel oxide)<sup>[6–11]</sup>. The use of dyes with complementary absorption properties enhances the light harvesting<sup>[12]</sup>. The structure of the sensitizer, along with the widening of the absorption band<sup>[13]</sup> from the visible to the NIR region, plays a crucial role to maximize the photocurrent and the overall efficiency in DSSCs. To our knowledge, few NIR absorbing dyes have been proposed, so far, for the sensitization of nickel oxide photocathodes<sup>[14–17]</sup>. Squaraines are well known for their sharp and intense absorption in the NIR region of the spectrum<sup>[18]</sup>. In 2012, Chang et al. proposed a series of triphenylamino-based squaraines with different anchoring groups as sensitizers in *p*-DSSCs reaching efficiencies up to 0.113%.<sup>[19]</sup> More recently, a new class of diphenylamino-substituted, indole-based squaraines has been investigated for the sensitization of nickel oxide as cathode of *p*-DSSCs<sup>[20,21]</sup>. Four types of squaraines with different symmetry were synthesized (Figure 1). These differed for the number of anchoring groups and the pattern of substitution on the squaric acid unit with electron-withdrawing groups as substituents (CN2, CN4, Figure 1). The high number of carboxylic groups in the symmetrical structures (O4, CN4), as well as the *cis*-conformation forced by the presence of dicyanovinyl-substituted squaric core (CN2, CN4), allowed better charge injection and recombination. To further explore the electron transfer directionality in the unsymmetrical structures, the chain-length on the indolenine nitrogen was varied in the series<sup>[22,23]</sup>.

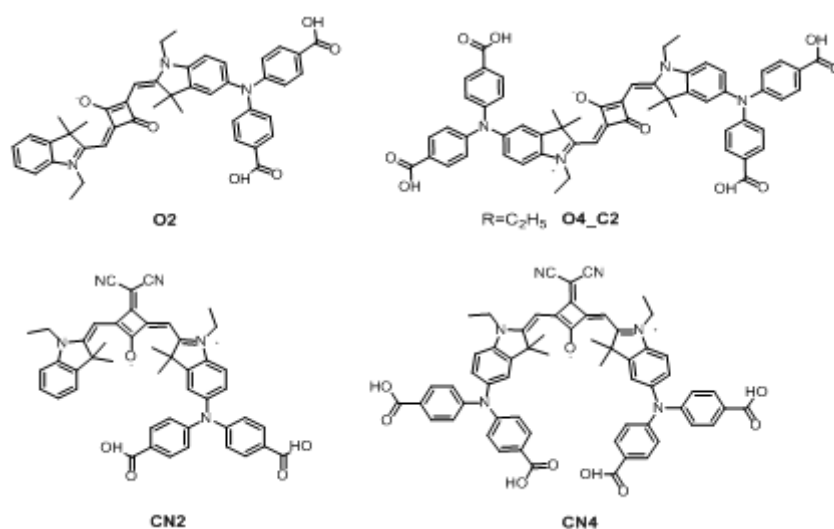
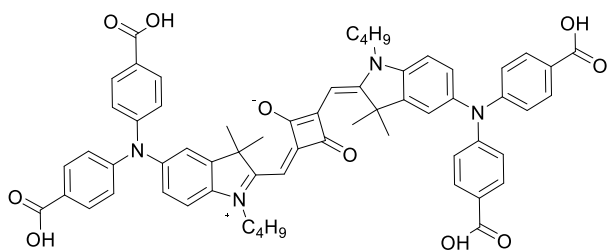
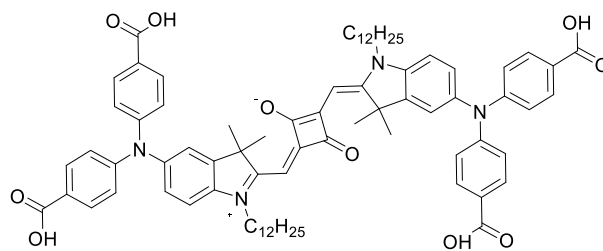


Figure 1. Diphenylamino-substituted squaraines.

Based on the promising result obtained by the symmetrical squaraine **O4\_C2**, the two novel squaraines **O4\_C4** and **O4\_C12** (Figure 2) were synthesized and considered as sensitizers of NiO photocathode for *p*-DSSC applications. These possess a longer alkyl chain as substituent of the isoindoline N atom when compared to parent **O4\_C2** (Figure 1).



**O4\_C4**



**O4\_C12**

Figure 2. Structure of the two novel squaraines **O4\_C4** and **O4\_C12** investigated in this work.

The length of the alkyl substituents in squaraines is known to affect their solubility in organic solvents<sup>[24]</sup> and their tendency to form aggregates<sup>[25–27]</sup> when the squaraines are chemisorbed on oxide surfaces. Beside the analysis of the performance of the p-DSSCs sensitized with **O4\_C4** and **O4\_C12** in this work we also explore the influence of NiO<sub>x</sub> surface pretreatment with NaOH prior to the step of electrode sensitization. The purpose of such a part of investigation is to reduce the acidity of the NiO surface which is responsible for the short-time stability of the devices. Moreover, it was found that NaOH can induce a partial transformation of the surface-localized Ni(III) sites into Ni(II). As very recently stressed by D’Amario and coworkers<sup>[28]</sup>, this reaction could enhance the overall efficiency of the device by minimizing the unwanted recombination phenomena occurring at the electrode/electrolyte interface.

## Results and Discussion

### Synthesis and spectroscopic properties of O4 dyes

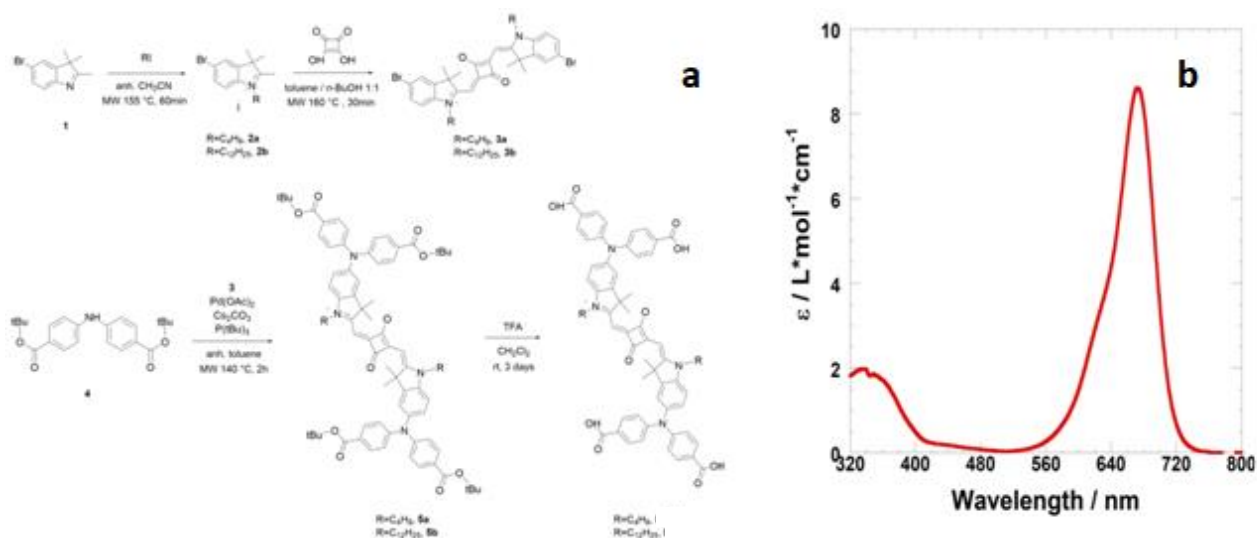


Figure 3. Left (a): scheme of the synthesis of squaraines **O4\_C4** and **O4\_C12**. Right (b): UV spectra of **O4\_C12** in ethanol.

Compounds **1**, **2a**, **2b**, **3a**, **3b**, **4**, **5a**, **5b** and **O4\_C2** (O4) were synthesized according to the literature<sup>[18]</sup>. **O4\_C4** and **O4\_C12** were obtained by simple hydrolysis in acidic conditions from their *tert*-butyl esters derivatives. The overall synthetic route is reported in Figure 3. Intense absorption is one of the key features of a dye for being used as sensitizer in a DSSC. Another relevant characteristic of the sensitizer is the amount that can be loaded onto the surface of a DSSC photoelectrode. Data in Table 1 clearly indicated that the increase of the alkyl chain length in the **O4** series, augmented the molar extinction coefficient in correspondence of the maximum of absorption ( $\epsilon$ ).

	<b>O4_C2</b>	<b>O4_C4</b>	<b>O4_C12</b>
$\epsilon / \text{L} \cdot \text{mol}^{-1} \cdot \text{cm}^{-1}$	<b>76 646</b>	<b>79 335</b>	<b>86 244</b>
HOMO level / V vs NHE	<b>0.64</b>	<b>0.63</b>	<b>0.64</b>
LUMO level / V vs NHE	<b>-0.81</b>	<b>-0.82</b>	<b>-0.80</b>

Table 1. Molar extinction coefficient ( $\epsilon$ ) at the wavelength of maximum absorption in ethanol and HOMO and LUMO levels. NHE : normal hydrogen electrode. HOMO and LUMO energy levels were calculated as reported in ref. <sup>[21]</sup>.

In Table 1, the positions of the HOMO/LUMO levels for the series of **O4** colorants are also displayed. The frontier energy levels are very similar for the **O4** series here considered due to the analogous extension of the network of electronic conjugation and the scarce dependence of these properties on the size of alkyl pending groups<sup>[29,30]</sup>.

#### Characterization of **O4**-sensitized NiO electrodes

When NiO<sub>x</sub> is sensitized with the dyes of the **O4** series we observe that the increase of the alkyl chain length reduces the amount of loaded dye (Table 2).

	<b>O4_C2</b>	<b>O4_C4</b>	<b>O4_C12</b>
Dye loading / mol cm <sup>-2</sup>	<b>1.12 * 10<sup>-8</sup></b>	<b>0.87 * 10<sup>-8</sup></b>	<b>0.35 * 10<sup>-8</sup></b>
Dye loading with NaOH / mol cm <sup>-2</sup>	<b>0.81 * 10<sup>-8</sup></b>	<b>0.76 * 10<sup>-8</sup></b>	<b>0.29 * 10<sup>-8</sup></b>

Table 2. Values of dye loading on pristine NiO and NaOH treated NiO.

The latter effect might be due to higher steric hindrance for the C12 derivative in comparison to the C2 and C4 functionalized ones. The length of the alkyl chain played a crucial role to reduce the aggregation phenomena, as detected by the appearance of a blue-shifted shoulder in the UV-vis spectra of the derivatives<sup>[31,32]</sup>. Direct comparison of the UV-vis spectra of **O4\_C2** and **O4\_C12** evidences the relative difference in the shoulder intensity. This finding stresses out the importance of using longer alkyl chains to reduce intermolecular aggregation. For the prevention of the latter phenomenon co-adsorbents such as chenodeoxycholic acid (CDCA) in the solution of sensitization are also used<sup>[33,34]</sup>. Nevertheless the presence of CDCA lowers the overall cell efficiency as reported for an analogue series of squaraines<sup>[23]</sup>. The surface pretreatment with NaOH sensibly reduced dye loading (Table 2) due to the competition between hydroxyl ions (OH<sup>-</sup>) and the carboxylic groups of the squaraines in the process of NiO<sub>x</sub> surface binding in correspondence of the Ni(III) sites. Previous studies with the technique of X-rays photoelectron spectroscopy (XPS) have demonstrated that pristine nickel oxide possesses nickel centres with states of oxidation +2 and +3<sup>[35,36]</sup>. The defective Ni(III) sites are mostly localized on the surface of the oxide and represent the sites of anchoring of the dye-sensitizer by virtue of the strong electrophilic character which favours anion adsorption.<sup>[37]</sup> Moreover, Ni(III) sites interaction very strongly with the basic moiety -CO<sub>2</sub><sup>-</sup> of the dye<sup>[38,39]</sup>. Based on these findings, it is reasonable to assume that the reaction of nickel oxide with NaOH will mostly consist in the binding of the hydroxide anion to Ni(III) centres with consequent decrease of the surface sites actually available for dye-anchoring. Therefore, it results that OH<sup>-</sup> anions compete with

the carboxylate anions of the squaraines in the process of occupation of the Ni(III) centres situated on oxide surface. In general, NaOH surface treatment brings about a decrease of dye-loading. This effect was particularly evident for **O4\_C2**, i.e. the dye which is loaded by NiO at the higher concentration.

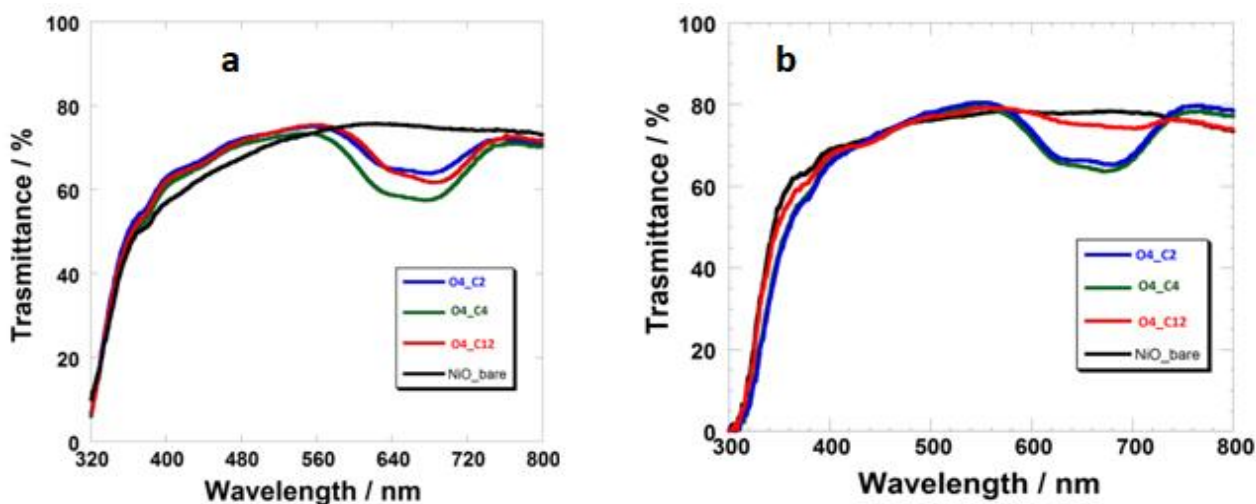


Figure 4. Transmittance spectra of **O4** sensitized NiO films with (right, b) and without (left, a) NaOH pretreatment. Spectral profiles of **O4\_C2**-, **O4\_C4**- and **O4\_C12**- sensitized NiO are in green, blue and red, respectively.

Transmittance spectra of sensitized NiO films (Figure 4) were consistent with the data of dye loading (Table 2). Transmittance at 360 nm, i.e. the absorption wavelength characteristic of defective NiO, rose up from 45% up to 60% as a consequence of the alkali treatment (Figure 4). Both untreated and alkali pre-treated films of bare NiO<sub>x</sub> have been used as photocathodes of a *p*-DSSC. The *p*-DSSC sensitized with **O4\_C2** showed the better conversion performance (0.035 %) with a cathodic current density approaching 1 mA cm<sup>-2</sup> (Figure 5 and data in Table 3). A slightly lower efficiency was determined with the *p*-DSSC sensitized with **O4\_C4** whereas the device with **O4\_C12** gave the worst conversion performance (Table 3). Generally, the worse performances were recorded for all the devices pretreated for 2 hours in NaOH solution ([NaOH] = 0.1 M).

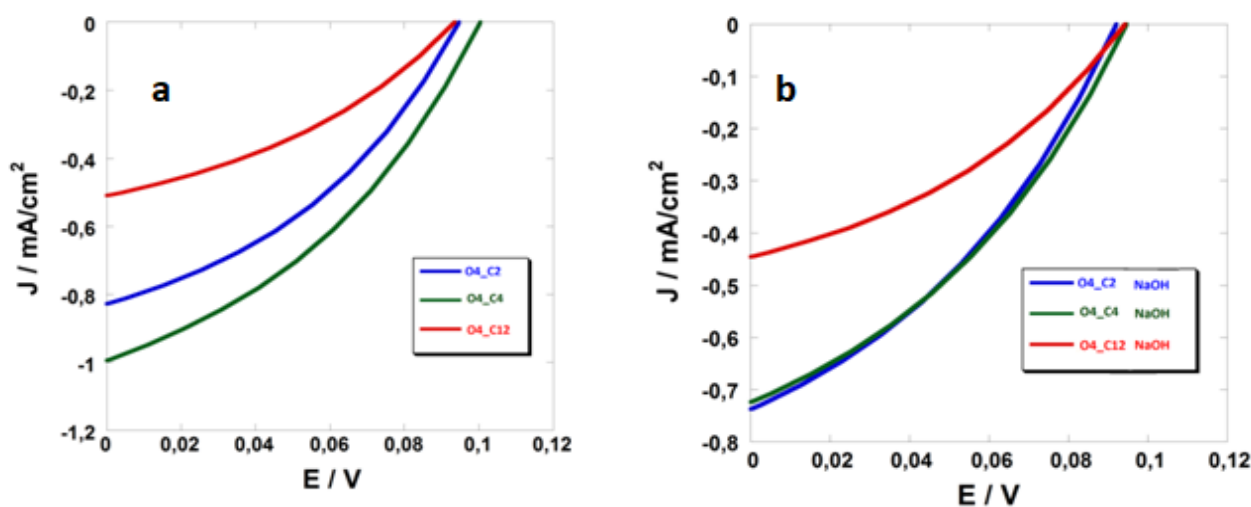


Figure 5. *JV* curves of the *p*-DSSCs sensitized with **O4** dyes. Right, b: *JV* curves obtained when NiO electrode was treated with NaOH. Left, a: *JV* curves obtained when NiO electrode was not treated with NaOH. The characteristic curves of the *p*-DSSCs with **O4\_C2**-, **O4\_C4**- and **O4\_C12**-sensitized NiO photocathodes are in green, blue and red, respectively.



Dye	$V_{oc}$ (mV)	$J_{sc}$ (mA/cm <sup>2</sup> )	FF (%)	$\eta$ (%)
O4_C2	99 ± 3	-0.980 ± 0.015	37.0 ± 0.2	0.035 ± 0.003
O4_C4	93 ± 4	-0.811 ± 0.022	37.6 ± 0.4	0.028 ± 0.002
O4_C12	92 ± 3	-0.486 ± 0.026	36.5 ± 0.3	0.016 ± 0.002
O4_C2*	92 ± 3	-0.702 ± 0.014	36.0 ± 0.1	0.023 ± 0.002
O4_C4*	91 ± 2	-0.696 ± 0.030	35.6 ± 0.4	0.020 ± 0.004
O4_C12*	92 ± 4	-0.416 ± 0.023	37.0 ± 0.2	0.013 ± 0.003

Table 3. Conversion efficiency parameters obtained from  $JV$  curves reported in Figure 5. Symbols  $V_{oc}$ ,  $J_{sc}$ , FF and  $\eta$  represent the open circuit voltage, the short-circuit current density, the fill factor and the overall conversion efficiency, respectively. \* Dye chemisorbed onto NiO surfaces that have treated with NaOH.

The open circuit voltage ( $V_{oc}$ ) as well as the fill factor (FF) of the  $p$ -DSSCs were the parameters less affected by the alkali pretreatment of the NiO cathode (Table 3). This is probably due to the weak reducing power of the hydroxyl anion which converts Ni(III) into Ni(II) thus diminishing the phenomenon of recombination between Ni(III) sites and iodide, i.e. the reduced form of the redox shuttle in the  $p$ -DSSCs device [28]. Therefore, the lower efficiency of the devices with soda treated photocathodes was mainly caused by the decrease of the photocurrent density. The detrimental effect of the alkali treatment was more pronounced for the cells sensitized with the dyes having the shorter length of the alkyl chain. The decrease of overall efficiency due to the soda treatment of the NiO<sub>x</sub> electrode was 32, 20 and 12% for **O4\_C2**, **O4\_C4** and **O4\_C12**, respectively. These values were in good agreement with the decrease of dye-loading in passing from non treated to soda treated NiO electrode (28, 13 and 17% respectively). The spectra of incident photon-to-current conversion efficiency (IPCE) were also recorded (Figure 6). The effect of sensitization of the three diverse squaraines of the **O4** series occurs in the range 580 and 750 nm, i.e. in correspondence of their optical absorption (see Figures 3 and 4 respectively for the absorption spectra of the squaraines in solution and in the surface immobilized state).

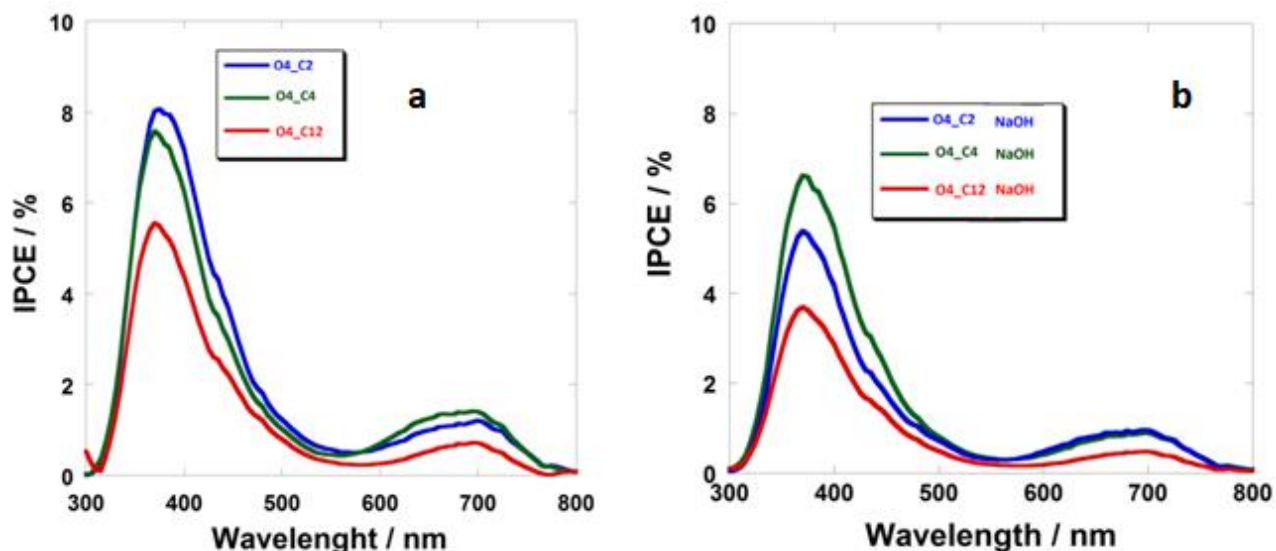


Figure 6. Left, a: IPCE spectra of the  $p$ -DSSCs at the condition of short circuit with non treated NiO photocathodes. Right, b: IPCE spectra of the  $p$ -DSSCs at the condition of short circuit with soda treated NiO photocathodes. The spectral profiles of the  $p$ -DSSCs with **O4\_C2**-, **O4\_C4**- and **O4\_C12**- sensitized NiO cathodes are shown in green, blue and red, respectively.

The lower values of IPCE of the cells with alkali treated NiO<sub>x</sub> cathodes are ascribed to the scarcer extent of dye loading (Table 2) combined to the generally poor properties of electron injection typical of squaraines-based devices<sup>[40]</sup>. All IPCE spectra (Figure 6) are characterized by a photocurrent peak at short wavelengths due to the intrinsic photoelectrochemical activity of NiO<sup>[40]</sup>, and a second broader peak at longer wavelength originated by the photoaction of the dye. It is worth nothing that the photocurrent peak at shorter wavelength typical of bare NiO<sub>x</sub> is significantly reduced by alkali treatment as a result of the decrease of Ni(III) sites.

### Electrochemical impedance spectroscopy of **O4**-sensitized *p*-DSSCs

Electrochemical impedance spectroscopy (EIS) has been employed as investigative technique to analyse how the electronic transport properties of the NiO electrode<sup>[41,42]</sup> are affected by the nature of the sensitizer and/or the alkali pretreatment. EI spectra (Figure 7) have been fitted with the model of equivalent circuit presented in refs.<sup>[43]</sup> and [36]. Fitting parameters are presented in Tables 3 and 4.

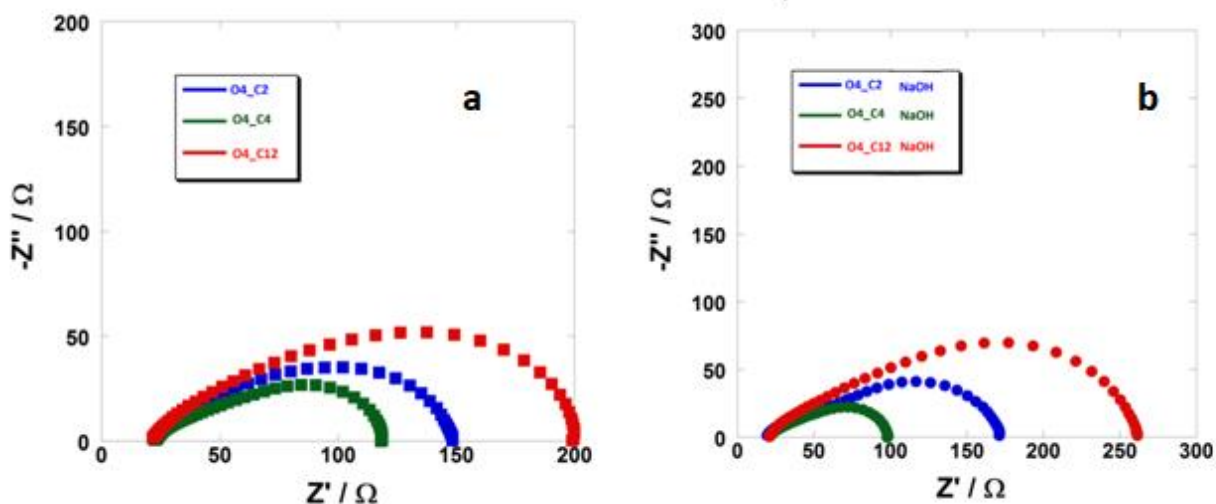


Figure 7. EIS spectra of illuminated *p*-DSSCs at the potential of open circuit with (left, a) non treated NiO photocathodes, and with (right, b) alkali treated NiO photocathodes.

The spectra of the *p*-DSSCs with **O4\_C2**-, **O4\_C4**- and **O4\_C12**- sensitized NiO electrodes are represented as green, blue and red dots, respectively. The values of charge transport resistance through **O4**-sensitized NiO film ( $R_t$ ), recombination resistance at the **O4**-sensitized NiO electrode/electrolyte interface ( $R_{rec}$ ), and chemical capacitance at the **O4**-sensitized NiO electrode/electrolyte interface ( $C_{\mu}$ ) are listed for the *p*-DSSCs with non treated (Table 4) and alkali treated (Table 5) NiO electrodes. Moreover, in Tables 4 and 5 the values of the parameters  $\tau_d$  (hole diffusion time),  $\tau_h$  (hole lifetime),  $L_h$  (diffusion length of the hole), and  $D_h$  (hole diffusion coefficient), which characterize the charge carriers photoinjected in NiO by the action of **O4** dye-sensitization, are also reported. The relationships between  $R_t$ ,  $R_{rec}$ ,  $C_{\mu}$  and  $\tau_h$ ,  $L_h$ ,  $D_h$  are described in ref. [39]. It is found that the transport resistance of the photoelectrode ( $R_t$  values in the second column from left in Tables 3 and 4) decreases upon increase of the short circuit current density and conversion efficiency ( $J_{sc}$  and  $\eta$  values in Table 3). Since  $R_t$  is inversely proportional to the concentration of the charge carriers photoinjected in NiO<sub>x</sub> [39], and a relatively large value of  $J_{sc}/\eta$  indicates a correspondingly high number of photoinjected charge carriers, it is expectable that  $R_t$  decreases with  $J_{sc}/\eta$ . Such a correlation between the ascending trend of  $J_{sc}/\eta$  and the descending trend of  $R_t$  holds also when NiO<sub>x</sub> cathode is treated with NaOH. It is recognized then that the length of the alkyl chain is a structural factor that generally inhibits the process of photoinjection since the enlargement of the substituent size accompanies the increase of  $R_t$ . This occurs for two principal reasons: i) as previously outlined, the increase of chain

length impedes the chemisorption of larger surface concentration of dye due to steric hindrance thus limiting the surface concentration of the photoactive units injecting charge into sensitized NiO<sub>x</sub>; ii) the alkyl chain, i.e. a functional unit with typically insulating properties, actually behaves as an agent of (photo)electrochemical passivation of the NiO<sub>x</sub> surface against charge photoinjection.

Dye	$R_t / \Omega$	$R_{rec} / \Omega$	$C_\mu / \text{mF}$	$\tau_d / \text{ms}$	$\tau_h / \text{ms}$	$L_h / \mu\text{m}$	$D_h / 10^{-6} \text{cm}^2 \text{s}^{-1}$
O4_C2	59.6 ± 11.3	66.4 ± 15.0	74 ± 19	4.41 ± 1.65	4.92 ± 2.36	2.11 ± 0.98	10.10 ± 1.97
O4_C4	98.1 ± 28.4	107.4 ± 34.2	81 ± 22	7.94 ± 4.45	8.70 ± 5.13	2.09 ± 1.00	5.50 ± 0.78
O4_C12	130.6 ± 22.7	135.5 ± 34.2	76 ± 22	9.87 ± 4.52	10.24 ± 5.5	2.04 ± 0.97	4.21 ± 0.54

Table 4. Transport and capacitive parameters obtained from the fitting of the photoelectrochemical impedance spectra of the devices with non alkali treated NiO electrodes.

Dye	$R_t / \Omega$	$R_{rec} / \Omega$	$C_\mu / \text{mF}$	$\tau_d / \text{ms}$	$\tau_h / \text{ms}$	$L_h / \mu\text{m}$	$D_h / 10^{-6} \text{cm}^2 \text{s}^{-1}$
O4_C2	54.3 ± 5.7	78.4 ± 7.9	73 ± 9	3.96 ± 0.90	5.72 ± 1.28	2.4 ± 0.4	14.5 ± 1.2
O4_C4	79.1 ± 6.6	184.0 ± 10.7	88 ± 9	6.96 ± 1.28	16.19 ± 2.3	3.1 ± 0.6	13.4 ± 1.0
O4_C12	193.4 ± 35.6	215.4 ± 33.5	121 ± 25	23.4 ± 9.1	26.0 ± 9.0	2.1 ± 0.7	1.9 ± 0.6

Table 5. Transport and capacitive parameters obtained from the fitting of the photoelectrochemical impedance spectra of the devices with alkali treated NiO electrodes.

When the term of recombination resistance of the photoelectrode is analysed ( $R_{rec}$  values in the third column from left in Tables 3 and 4), we observe that  $R_{rec}$  increases with the length (size) of the alkyl substituent. In a *p*-DSSC the parameter  $R_{rec}$  is an electrical term that refers to the difficulty with which the iodide, i.e. the product of photoreduction, recombines chemically with the holes photoinjected in NiO<sub>x</sub>, i.e. the other product formed by the excited sensitizer after its regeneration [16]. The direct correlation between  $R_{rec}$  and substituent size in **O4** series reveals that the electrically insulating nature of the alkyl chain serves as protection of sensitized NiO<sub>x</sub> surface against charge recombination (desirable effect). This consideration is somewhat similar to the conclusions drawn in precedence when the trend of  $R_t$  was analysed in terms of the size of the alkyl chain for the **O4** series: in fact, it was recognized that the non conducting alkyl group acted also as a protection against charge photoinjection in NiO<sub>x</sub> (unwanted effect). The rate of the hole-iodide recombination (bimolecular event) is directly related to the concentration of I<sup>-</sup> at the electrode surface and the unbound Ni(III) sites on the NiO surface. The treatment with NaOH lowers the concentration of Ni(III) sites (as determined by the trend of dye-loading, Table 2), and leads to the eventual adsorption of hydroxyl anions that charge negatively the NiO<sub>x</sub> surface: this combination of processes would render less probable the event of recombination and disfavours energetically the adsorption of I<sup>-</sup>. Therefore, the synergic passivation effect created by a longer alkyl chain and the alkali pretreatment hamper the process of recombination between the unbound Ni(III) sites and iodide anions [44]. The recombination resistance is directly proportional to the lifetime of the holes photoinjected in NiO<sub>x</sub> [45] (compare trends of  $R_{rec}$  and  $\tau_h$  in Tables 4 and 5), with  $R_{rec}$  related to the cell parameter of open circuit potential [39]. Since the insulating action of the **O4** squaraines against photoinjection and charge recombination becomes more efficacious upon increase of alkyl chain size as testified by the increase of  $R_t$  and  $R_{rec}$  terms, the decrease of  $J_{SC}/\eta$  with the increase of alkyl chain size is offset by the quasi-constancy of the value of  $V_{OC}$  (Table 3). Therefore, the increase in the size of the alkyl substituent in the **O4** series reduces the surface concentration of dye-sensitizer, decreases consequently  $J_{SC}$  and  $\eta$ , but improves  $V_{OC}$  by

virtue of the electrically insulating properties of the alkyl group. The treatment of the NiO cathode with NaOH provokes the simultaneous increase of  $R_{rec}$  and  $\tau_h$  for the corresponding  $p$ -DSSCs sensitized by the **O4** series with respect to the devices in which NiO<sub>x</sub> cathodes were not treated with soda prior to sensitization (Tables 3 and 4). Since soda treatment is expected to decrease the number of surface Ni(III) sites, i.e. the species that react with the dye for its surface immobilization and, more importantly, are directly involved in the phenomenon of charge recombination (*vide supra*), such trends of  $R_{rec}$  and  $\tau_h$  are clearly consistent with the decrease of the surface concentration of the centres of recombination consequent to NaOH treatment.

The value of chemical capacitance at the photoelectrode/electrolyte interface is not affected by the nature of the sensitizer and its loading when NiO<sub>x</sub> electrode is not treated with alkali (see  $C_{\mu}$  values in the fourth column from left in Table 4). This implies that the charge distribution at the electrode/electrolyte interface, i.e. the physical entity that is characterized by the parameter of the capacitance, depends mainly on the nature of the NiO<sub>x</sub> substrate. As a matter of fact, the capacitance at the electrode/electrolyte interface is determined by the amount of charge separated at that interface [39]. Since  $C_{\mu}$  is practically constant for the three differently sensitized  $p$ -DSSCs (fourth column from left in Table 4) one has to expect that non-treated nickel oxide in the sensitized state possesses a surface concentration of free Ni(III) sites (i.e. the surface species that constitute the excess of charge at the electrode/electrolyte interface and determine the value of interfacial capacitance), which is considerably larger than the fraction of Ni(III) sites occupied by the anchored sensitizer. This conclusion stems from the fact that the differences of dye-loading on pristine NiO<sub>x</sub> (see Table 2) are not sufficiently large to determine a considerable variation of free Ni(III) sites, i.e. the surface centres that did not combine with the dye-sensitizer under the adopted conditions of sensitization. Due to the invariance of  $C_{\mu}$ , the trends of the diffusion time ( $\tau_d$ ), i.e. the time the photoinjected holes require to go throughout the NiO<sub>x</sub> film, and the holes lifetime ( $\tau_h$ ), i.e. the time the holes endure before an event of recombination or trapping occurs, follow respectively the trends of  $R_t$  and  $R_{rec}$ . Time values are straightforwardly calculated through the relationships that relate these parameters to the resistance and capacitance values determined by fitting the impedance spectra (Figure 7) <sup>[46,47]</sup>. On the other hand, it was evident that the treatment of NiO with alkali introduced differences among the values of chemical capacitance when the dye is varied ( $C_{\mu}$  values in the fourth column from left in Table 5).  $C_{\mu}$  increased with the size of the alkyl chain. This finding can be explained by considering that the larger the size of the anchored sensitizer the higher the number of anchoring sites adjacent to the site of anchoring which cannot be further occupied. The free sites would represent the actual centres that contribute to the determination of the excess of charge at the basis of the capacitance  $C_{\mu}$ . The dynamics of **O4** dye anchoring onto NiO surfaces would then follow the model of size-limited occupancy of anchoring sites which has been developed previously for the squaraines of the VG series [39]. When compared to the corresponding data in Table 4, the values of  $C_{\mu}$  generally increase after the treatment of NiO<sub>x</sub> with NaOH (Table 5). As previously observed during the discussion of the trends of dye-loading (Table 2), the alkali treatment of NiO decreases the surface concentration of the Ni(III) sites in correspondence of which dye-anchoring takes place. Such an inactivation of the Ni(III) sites employed for dye-anchoring can occur through two distinct (and eventually concomitant) processes: a) coordination of OH<sup>-</sup> anions by Ni(III) sites; b) chemical reduction of Ni(III) into Ni(II) with the concomitant oxidation of the hydroxyl ion. Since  $C_{\mu}$  generally increases with the alkali treatment, it is supposed that NaOH inactivates only a very small fraction of surface sites destined to dye anchoring but does not alter the surface concentration of the type of Ni(III) centres that form the excess of surface charge and determine the capacitance.

The hole diffusion length  $L_h$ , is generally longer than the nominal thickness of the electrode ( $l = 2 \mu\text{m}$ ) for all three sensitizers (Tables 4 and 5). Moreover, it poorly depends on the eventual application of soda pretreatment. This would indicate that only a negligible fraction of photoinjected holes tends to recombine

1 before reaching the collecting surface at FTO/NiO<sub>x</sub> interface. Since the value of  $L_h$  is quite independent on  
2 the transport and recombination properties of the photoelectrode, we can conclude that the hole diffusion  
3 length depends principally on the bulk properties of the NiO<sub>x</sub> film for this type of sensitized electrodes.

4  
5  
6  
7  
8  
9  
10  
11  
12  
13  
14  
15  
16  
17  
18  
19  
20  
21  
22  
23  
24  
25  
26  
27  
28  
29  
30  
31  
32  
33  
34  
35  
36  
37  
38  
39  
40  
41  
42  
43  
44  
45  
46  
47  
48  
49  
50  
51  
52  
53  
54  
55  
56  
57  
58  
59  
60  
61  
62  
63  
64  
65

When NiO<sub>x</sub> is not treated with soda, the diffusion coefficient  $D_h$  of the photoinjected holes through the sensitized oxide (Table 4) follows the trend of the overall efficiency and the short-circuit current density (Table 3), i.e.  $D_h$  increases on going from the device sensitized with **O4\_C12** to the  $p$ -DSSC employing **O4\_C2**. Dye-loading also increases on going from **O4\_C12** to **O4\_C2** (Table 2). This combination of findings leads to suppose that  $D_h$  is directly proportional to the amount of photoinjected charge carriers and the rate of injection. In passing from NiO<sub>x</sub> sensitized in pristine state to NiO sensitized after the treatment with alkali we observe a general increase of  $D_h$  values with the exception of the device sensitized with **O4\_C12** (Tables 4 and 5). Since overall efficiencies (Table 3) as well as dye-loading values (Table 2) diminish with alkali treatment, we attribute the increase of the diffusion coefficient of the photoinjected carriers to the amelioration of the electronic characteristics of NiO<sub>x</sub> after the treatment with NaOH. The reaction with hydroxide would result beneficial in removing defects from the surface of NiO<sub>x</sub>. Such defects would eventually act as trapping agents against the diffusion of the photoinjected charge carriers in the bulk of the oxide.

#### *Analysis of the stability of O4-sensitized p-DSSCs*

For the evaluation of the time-stability of the six different types of  $p$ -DSSCs here considered (Table 3), we adopted the standard procedure ISOS-D1<sup>[48]</sup> that is defined for the analysis of the degradation of photovoltaic cells stored in dark conditions. The  $p$ -DSSCs were kept outdoor in dark conditions. The cell parameters were recorded after 1, 2, 5, 10, 30 and 60 days from the date of fabrication. The ISOS-D1 standard procedure was selected to test the chemical stability of the squaraines on the NiO<sub>x</sub> surface. All characteristic parameters of the photoelectrochemical cells were recorded and averaged having considered five devices for each type of  $p$ -DSSC. The averaged values of  $V_{OC}$ ,  $J_{SC}$ , FF and  $\eta$  were plotted as a function of the time (Figure 8). After an initial improvement of the photoconversion properties during the first three days of dark storage<sup>[49]</sup>, all devices showed a progressive decay of all four parameters. After 60 days of dark storage the efficiency of the  $p$ -DSSCs decays to 70% of the starting one whereas the fill factor and the open circuit voltage decreased to about 95% of the initial values. The decreases of short-circuit current density and overall efficiency were more pronounced for the devices with non alkali treated photocathodes. Both types of **O4\_C2** sensitized devices displayed the better performances for the whole duration of time-stability experiment with respect to the other four devices sensitized with **O4\_C4** and **O4\_C12** (Figure 8). The alkali treatment of the photocathode did not alter the relative trends of the parameters characterizing the **O4\_C2** sensitized devices whereas the  $p$ -DSSCs sensitized with **O4\_C4** and **O4\_C12** showed changes of parameters that led to the same steady-state values after two months of dark storage (Figure 8). In case of **O4\_C4** and **O4\_C12** sensitized devices it is believed that the reach of a common value is a consequence of the complete detachment of the squaraine sensitizers. The effect of colorant detachment is then more evident for the cells employing the two squaraines **O4\_C4** and **O4\_C12**, i.e. the sensitizers with the lowest values of dye-loading (Table 2).

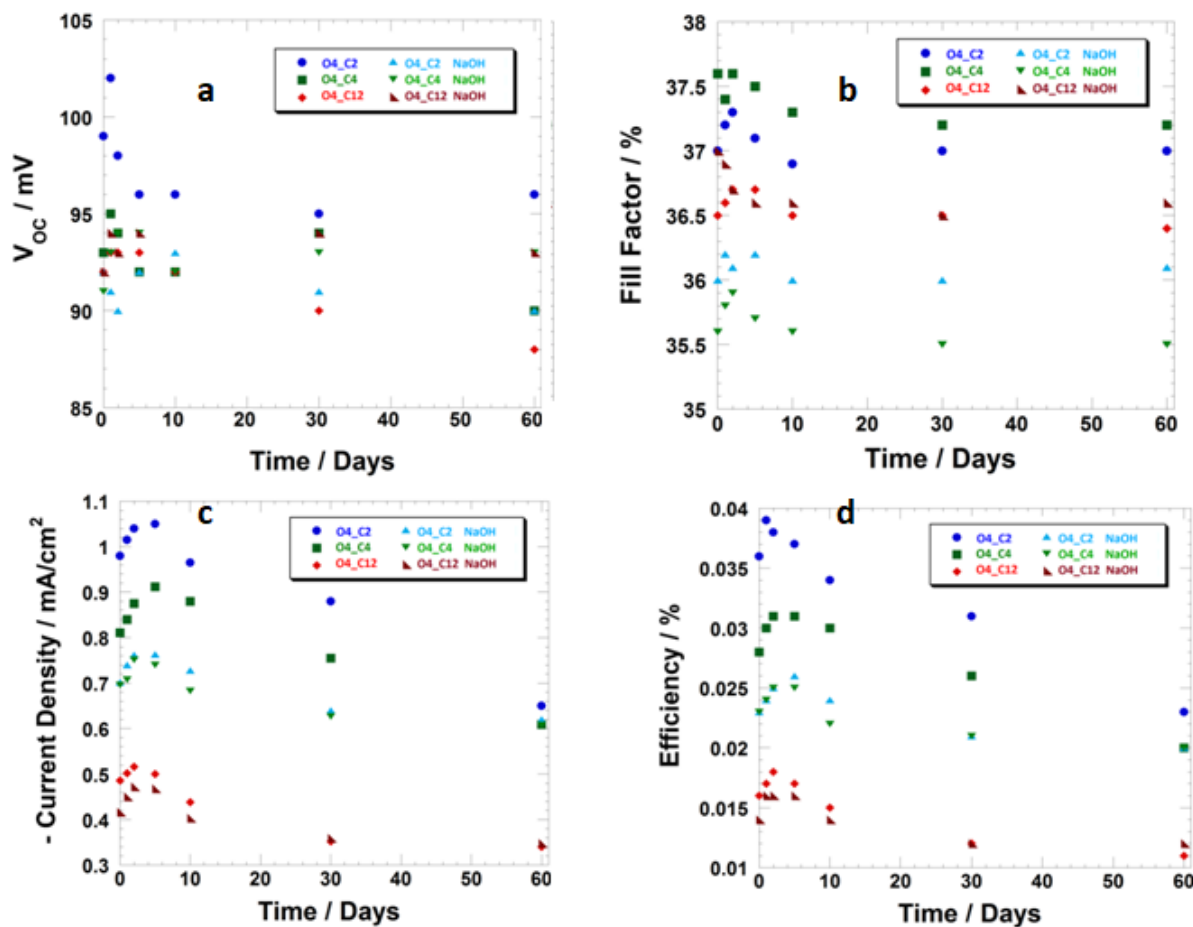


Figure 8. Temporal variation of the four main parameters of the six different types of photoelectrochemical cells here considered. The values reported in the graphs are averages that have been calculated from the parameters of five devices for each type. For the realization of the experiment of time stability have been employed thirty cells.

## Conclusions

Three different squaraines of the **O4** series (Figures 1 and 2) were synthesized and characterized. These molecules differed for the length of the alkyl substituent [ $-C_2H_5$  (**O4\_C2**),  $-C_4H_9$  (**O4\_C4**),  $-C_{12}H_{25}$  (**O4\_C12**)] while the extent of electronic conjugation remained the same as verified by the quasi-constancy of the HOMO-LUMO levels (ca. 0.60 and -0.80 V vs NHE for HOMO and LUMO, respectively) and the wavelength of maximum optical absorption (ca. 670 nm). The use of **O4\_C2**, **O4\_C4** and **O4\_C12** as dye-sensitizers of NiO<sub>x</sub> photocathodes in *p*-DSSCs was evaluated comparatively. The length of the alkyl pending groups affected the extent of loading on NiO surface with dramatic consequences on the efficiency of photoconversion in the differently sensitized devices. The photoelectrochemical cells that employed **O4\_C2**, i.e. the dye with the shorter chain length, displayed the largest efficiencies (0.035%) with a maximum of external quantum efficiency of about 1.5% in the range of absorption of surface immobilized **O4\_C2**. In this work the effect of the alkali treatment of NiO photocathodes on the photoconversion properties of the corresponding *p*-DSSCs has been also analysed. The treatment of NiO<sub>x</sub> with NaOH leads to the general decrease of the efficiency of conversion in the corresponding *p*-DSSCs due mainly to a diminution of the sites available to the dye for anchoring regardless of the nature of squaraine sensitizer. This conclusion was drawn after having measured the diminution of dye-loading for all three squaraines following the alkalisation of NiO<sub>x</sub> surface. Such an effect has been ascribed to the action of passivation that the hydroxyl anion would exert

350 on the Ni(III) centres, i.e. the sites of dye-anchoring on oxide surface. The identification of the actual  
1 reaction of Ni(III) passivation by soda requires further investigation with surface spectroscopic techniques.  
2 Electrochemical impedance spectroscopy has revealed that the overall efficiency  $\eta$  of the cell is directly  
3 related to the electrical parameter of transport resistance  $R_t$  through the NiO electrode with  $\eta$  increasing  
4 upon decrease of  $R_t$ . At the microscopic level a high diffusion coefficient of the photoinjected charge  
5 carriers results beneficial for the amelioration of the photoelectrochemical characteristics of the cell.  
6  
355 Finally, a study of the time-stability of the variously sensitized cells was conducted over a range of 60 days  
8 following the standard procedure ISOS-D1. After an initial improvement of the conversion properties  
9 during the first three days of test, cells underwent to a continuous process of degradation with the reach of  
10 a steady state after one month. Degradation was ascribed to the progressive detachment of the dye.  
11  
12  
13  
14

## 360 Supporting Information Summary

15 In the Supporting Information the experimental procedures are reported: details of the synthesis of **O4\_C4**  
16 and **O4\_C12**; device assembly and characterization.  
17  
18  
19  
20

## 365 Acknowledgments

21 Authors thank Dr. Davide Saccone for the suggestions given during the realization of some  
22 synthetic steps.  
23  
24  
25  
26

## 27 Keywords

28 Nickel Oxide; NIR-adsorber; p-type DSSC; Squaraines.  
29  
30  
31  
32  
33  
34

## 35 References

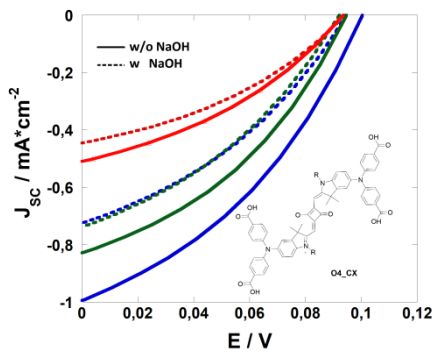
- 35 [1] B. O'Regan, M. Gratzel, *Nature* **1991**, 353, 737.  
36 [2] K. Kakiage, Y. Aoyama, T. Yano, K. Oya, J. Fujisawa, M. Hanaya, *Chem. Commun.* **2015**, 51, 15894–  
37 15897.  
38 [3] P. Ho, S. Thogiti, Y. H. Lee, J. H. Kim, *Sci. Rep.* **2017**, 7, 2272.  
39 [4] M. K. Nazeeruddin, P. Péchy, T. Renouard, S. M. Zakeeruddin, R. Humphry-Baker, P. Cointe, P. Liska,  
40 L. Cevey, E. Costa, V. Shklover, et al., *J. Am. Chem. Soc.* **2001**, 123, 1613–1624.  
380 [5] J. N. Clifford, A. Forneli, H. Chen, T. Torres, S. Tan, E. Palomares, *J. Mater. Chem.* **2011**, 21, 1693–  
42 1696.  
43 [6] J. He, H. Lindström, A. Hagfeldt, S.-E. Lindquist, *J. Phys. Chem. B* **1999**, 103, 8940.  
44 [7] D. Xiong, W. Chen, *Front. Optoelectron.* **2012**, 5, 371–389.  
45 [8] H. Choi, T. Hwang, S. Lee, S. Nam, J. Kang, B. Lee, B. Park, *J. Power Sources* **2015**, 274, 937.  
385 [9] C. J. Wood, G. H. Summers, C. A. Clark, N. Kaeffer, M. Braeutigam, L. R. Carbone, L. D'Amario, K. Fan,  
48 Y. Farré, S. Narbey, et al., *Phys. Chem. Chem. Phys.* **2016**, 18, 10727.  
49 [10] M. Awais, E. Gibson, J. G. Vos, D. P. Dowling, A. Hagfeldt, D. Dini, *ChemElectroChem* **2014**, 1, 384.  
50 [11] M. Awais, D. D. Dowling, M. Rahman, J. G. Vos, F. Decker, D. Dini, in *J. Appl. Electrochem.*, **2013**, pp.  
51 191–197.  
390 [12] Z. Ji, G. Natu, Z. Huang, O. Kokhan, X. Zhang, Y. Wu, *J. Phys. Chem. C* **2012**, 116, 16854–16863.  
54 [13] P. Qin, J. Wiberg, E. A. Gibson, M. Linder, L. Li, T. Brinck, A. Hagfeldt, B. Albinsson, L. Sun, *J. Phys.*  
55 *Chem. C* **2010**, 114, 4738–4748.  
56 [14] M. Bonomo, A. Carella, R. Centore, A. Di Carlo, D. Dini, *J. Electrochem. Soc.* **2017**, 164, F1412–F1418.  
57 [15] Y. Farré, L. Zhang, Y. Pellegrin, A. Planchat, E. Blart, M. Boujtita, L. Hammarstrom, D. Jacquemin, F.  
58 Odobel, *J. Phys. Chem. C* **2016**, 120, 7923–7940.  
395 [16] M. Bonomo, D. Dini, *Energies* **2016**, 9, DOI 10.3390/en9050373.  
60  
61  
62  
63  
64  
65

- 1  
2  
3  
4  
5  
6  
7  
8  
9  
10  
11  
12  
13  
14  
15  
16  
17  
18  
19  
20  
21  
22  
23  
24  
25  
26  
27  
28  
29  
30  
31  
32  
33  
34  
35  
36  
37  
38  
39  
40  
41  
42  
43  
44  
45  
46  
47  
48  
49  
50  
51  
52  
53  
54  
55  
56  
57  
58  
59  
60  
61  
62  
63  
64  
65
- [17] D. Ameline, S. Diring, Y. Farre, Y. Pellegrin, G. Naponiello, E. Blart, B. Charrier, D. Dini, D. Jacquemin, F. Odobel, *RSC Adv.* **2015**, *5*, 85530–85539.
- [18] N. Barbero, C. Magistris, J. Park, D. Saccone, P. Quagliotto, R. Buscaino, C. Medana, C. Barolo, G. Viscardi, *Org. Lett.* **2015**, *17*, 3306.
- [19] C. H. Chang, Y. C. Chen, C. Y. Hsu, H. H. Chou, J. T. Lin, *Org. Lett.* **2012**, *14*, 4726.
- [20] G. Naponiello, I. Venditti, V. Zardetto, D. Saccone, A. Di Carlo, I. Fratoddi, C. Barolo, D. Dini, *Appl. Surf. Sci.* **2015**, *356*, 911–920.
- [21] O. Langmar, D. Saccone, A. Amat, S. Fantacci, G. Viscardi, C. Barolo, R. D. Costa, D. M. Guldi, *ChemSusChem* **2017**, *10*, 2385–2393.
- [22] M. . Bonomo, D. . Saccone, C. . Magistris, A. . Di Carlo, C. . Barolo, D. Dini, *ChemElectroChem* **2017**, *4*, 2385–2397.
- [23] M. Bonomo, D. Saccone, C. Magistris, C. Barolo, L. Ciná, A. Di Carlo, D. Dini, *J. Electrochem. Soc.* **2017**, *164*, H1099–H1111.
- [24] C. Zheng, I. Jalan, P. Cost, K. Oliver, A. Gupta, S. Misture, J. A. Cody, C. J. Collison, *J. Phys. Chem. C* **2017**, *121*, 7750–7760.
- [25] A. J. McKerrow, E. Buncl, P. M. Kazmaier, *Can. J. Chem.* **1995**, *73*, 1605–1615.
- [26] G. Chen, H. Sasabe, Y. Sasaki, H. Katagiri, X. F. Wang, T. Sano, Z. Hong, Y. Yang, J. Kido, *Chem. Mater.* **2014**, *26*, 1356–1364.
- [27] G. M. Paternò, L. Moretti, A. J. Barker, C. D’Andrea, A. Luzio, N. Barbero, S. Galliano, C. Barolo, G. Lanzani, F. Scotognella, *J. Mater. Chem. C* **2017**, *5*, 7732–7738.
- [28] L. D’Amario, R. Jiang, U. B. Cappel, E. A. Gibson, G. Boschloo, H. Rensmo, L. Sun, L. Hammarström, H. Tian, *ACS Appl. Mater. Interfaces* **2017**, *9*, 33470–33477.
- [29] D. Joly, M. Godfroy, L. Pellejà, Y. Kervella, P. Maldivi, S. Narbey, F. Oswald, E. Palomares, R. Demadrille, *J. Mater. Chem. A* **2017**, *5*, 6122–6130.
- [30] T. Higashino, K. Kawamoto, K. Sugiura, Y. Fujimori, Y. Tsuji, K. Kurotobi, S. Ito, H. Imahori, *ACS Appl. Mater. Interfaces* **2016**, *8*, 15379–15390.
- [31] S. Maniam, A. B. Holmes, G. A. Leeke, A. Bilic, G. E. Collis, *Org. Lett.* **2015**, *17*, 4022–4025.
- [32] J. H. Yum, S. J. Moon, R. Humphry-Baker, P. Walter, T. Geiger, F. Nüesch, M. Grätzel, M. D. K. Nazeeruddin, *Nanotechnology* **2008**, *19*, 424005.
- [33] P. Salvatori, G. Marotta, A. Cinti, C. Anselmi, E. Mosconi, F. De Angelis, *J. Phys. Chem. C* **2013**, *117*, 3874–3887.
- [34] L. Favereau, Y. Pellegrin, L. Hirsch, A. Renaud, A. Planchat, E. Blart, G. Louarn, L. Cario, S. Jobic, M. Boujtita, et al., *Adv. Energy Mater.* **2017**, *7*, 1601776.
- [35] A. G. Marrani, V. Novelli, S. Sheehan, D. P. Dowling, D. Dini, *ACS Appl. Mater. Interfaces* **2014**, *6*, 143–152.
- [36] M. Bonomo, A. G. Marrani, V. Novelli, M. Awais, D. P. Dowling, J. G. Vos, D. Dini, *Appl. Surf. Sci.* **2017**, *403*, DOI 10.1016/j.apsusc.2017.01.202.
- [37] M. Bonomo, D. Dini, A. G. Marrani, *Langmuir* **2016**, *32*, DOI 10.1021/acs.langmuir.6b03695.
- [38] M. Bonomo, D. Dini, A. G. Marrani, R. Zaroni, *Colloids Surfaces A Physicochem. Eng. Asp.* **2017**, DOI 10.1016/j.colsurfa.2017.04.029.
- [39] M. Bonomo, F. Sabuzi, A. Di Carlo, V. Conte, D. Dini, P. Galloni, *New J. Chem.* **2017**, *41*, 2769–2779.
- [40] M. Bonomo, N. Barbero, F. Matteocci, A. Di Carlo, C. Barolo, D. Dini, *J. Phys. Chem. C* **2016**, *120*, 16340–16353.
- [41] D. Dini, Y. Halpin, J. G. Vos, E. A. Gibson, *Coord. Chem. Rev.* **2015**, *304–305*, 179–201.
- [42] M. Awais, M. Rahman, J. M. Don MacElroy, D. Dini, J. G. Vos, D. P. Dowling, *Surf. Coatings Technol.* **2011**, *205*, S245–S249.
- [43] M. Bonomo, G. Naponiello, I. Venditti, V. Zardetto, A. Di Carlo, D. Dini, *J. Electrochem. Soc.* **2017**, *164*, H137–H147.
- [44] S. Sheehan, G. Naponiello, F. Odobel, D. P. Dowling, A. Di Carlo, D. Dini, *J. Solid State Electrochem.* **2015**, *19*, 975–986.
- [45] E. A. Gibson, M. Awais, D. Dini, D. P. Dowling, M. T. Pryce, J. G. Vos, G. Boschloo, A. Hagfeldt, *Pccp* **2013**, *15*, 2411–2420.



- 450 [46] J. Bisquert, *J. Phys. Chem. B* **2002**, *106*, 325.  
1 [47] Á. Pitarch, G. Garcia-Belmonte, I. Mora-Seró, J. Bisquert, *Phys. Chem. Chem. Phys.* **2004**, *6*, 2983–  
2 2988.  
3 [48] M. O. Reese, S. A. Gevorgyan, M. Jørgensen, E. Bundgaard, S. R. Kurtz, D. S. Ginley, D. C. Olson, M. T.  
4 Lloyd, P. Morvillo, E. A. Katz, et al., *Sol. Energy Mater. Sol. Cells* **2011**, *95*, 1253–1267.  
5 [49] D. Pumiglia, M. Giustini, D. Dini, F. Decker, A. Lanuti, S. Mastroianni, S. Veyres, F. Caprioli,  
455 *ChemElectroChem* **2014**, *1*, 1388.  
6  
7  
8  
9  
10  
11  
12  
13  
14  
15  
16  
17  
18  
19  
20  
21  
22  
23  
24  
25  
26  
27  
28  
29  
30  
31  
32  
33  
34  
35  
36  
37  
38  
39  
40  
41  
42  
43  
44  
45  
46  
47  
48  
49  
50  
51  
52  
53  
54  
55  
56  
57  
58  
59  
60  
61  
62  
63  
64  
65

## Table Of Contents



J-V curves of treated (dotted line) and untreated (solid line) electrode with different squarainic sensitizers. The effect of soda pretreatment is to reduce the overall efficiency because of the adsorption competition between hydroxyl moiety of soda and carboxylic group of the sensitizers. Nevertheless, NaOH pretreatment enhance the long term stability of the devices (ISO-D1, more than 60 days) no matter the sensitizer employed.

